Mediators of mechanotransduction between bone cells

Problem Presenter: Svetlana V. Komarova (McGill University)

Contributors: Luciano Buono (UOIT), Svetlana V. Komarova (McGill University), Monserratt Lopez (McGill University), Robert M. Miura (NJIT), Adam Pan (University of Toronto), Mary Pugh (University of Toronto), Sanjive Qazi (Gustavus Adolphus College), David J.N. Wall (University of Canterbury, NZ), Thomas J.W. Wright (Hospital for Sick Children)

Report prepared by[1]**:** S.V. Komarova, M. Lopez, R.M. Miura, S. Qazi, and D.J.N. Wall.

1 Introduction

Mechanical forces are known to regulate the function of tissues in the body, including bone. Bone adapts to its mechanical environment by altering its shape and increasing its size in response to increases in mechanical load associated with exercise, and by decreasing its size in response to decreases in mechanical load associated with microgravity or prolonged bed rest [8]. Changes in bone size and shape are produced by a cooperative action of two main types of the bone cells - osteoclasts that destroy bone and osteoblasts that build bone [7]. These cell types come from different developmental origins, and vary greatly in their characteristics, such as size, shape, and expression of receptor subtypes, which potentially may affect their responses to mechanical stimuli [4]. The objective of this study is to compare the responses of osteoclasts and osteoblasts to mechanical stimulation.

2 Experimental Setup

Bone marrow cells were isolated and plated on a glass-bottom culture dish. The cultures were treated for 4-8 days with ascorbic acid to induce osteoblast differentiation and with RANKL to induce osteoclast differentiation. On the days of the experiments, each dish was first loaded with calcium-sensitive dye fura-2, then the dye was washed out and the dish was placed on the microscope stage. A single cell in the field was identified as an osteoblast or osteoclast based on its morphological features - osteoblasts are small spindle-shaped mononucleated cells and osteoclasts are large cells of 30-60 μm in diameter that contain more than 2 nuclei. Changes in emission at 510 nm following alternating illumination at 340 and 380 nm were recorded, from which cytosolic free calcium concentrations $[\mathsf{Ca}^{2+}]_i$ were later

[1] svetlana.komarova@mcgill.ca, lopezm@physics.mcgill.ca, miura@njit.edu, sqazi@gustavus.edu, d.wall@math.canterbury.ac.nz

calculated based on a calibration. For each experiment, after 10 s of basal recording, a single osteoclast or osteoblast (primary cell) was gently touched by a micropipette (mechanical stimulation) and changes in $[\mathsf{Ca}^{2+}]_i$ in the primary cell as well as other cells in the field (secondary cells) were recorded over 80-120 s. In response to the mechanical stimulation, the primary cell exhibited an increase in $[\mathsf{Ca}^{2+}]_i$ that was fast at the onset and then declined relatively slowly. In the neighbouring cells, delayed elevations in $[\mathsf{Ca}^{2+}]_i$ were observed consistent with a release of a mediator(s) from a primary cell. To examine if the nature of a mediator can be identified from these experiments, 3 independent recordings with an osteoblast as the primary cell and 5 independent recordings with an osteoclast as the primary cell were analyzed.

3 Analysis and Modelling

3.1 Data analysis of osteoblast and osteoclast recordings. For each experiment, the following information was available:

1. The geographic location of different cells.
2. The temporal dependence of $[\mathsf{Ca}^{2+}]_i$ in the primary and secondary responders.

From these data we have assessed the following parameters:

1. The distance R between the centroids of the primary (stimulated) and each of the secondary cells.
2. The time t between the onset of $[\mathsf{Ca}^{2+}]_i$ elevation in the primary cell and in each of the secondary responders.
3. The apparent diffusion coefficient (R^2/t) for each secondary responder.
4. The maximum amplitudes of $[\mathsf{Ca}^{2+}]_i$ in the primary and secondary responses.
5. The frequency and power of the oscillatory component present in the secondary responders.

Analysis of covariance (ANCOVA) was performed to assess the significance of the distance and the experimental factors on the apparent diffusion coefficient. In the model, the distance factor was the co-variate on the experimental factor, and an interaction term was included to determine if any effect of distance was dependent on the experiment. We log transformed the apparent diffusion coefficient measurement for each cell response to homogenize the group variance and normalize the scatter around the line of best fit. The null hypothesis was that the apparent diffusion coefficient will not be different between experiments and will be consistent for all cell responses for all distances from the source. To test for significance of the departure from the null hypothesis, an F-test with an F-distribution was used to compare statistical models. The probability value P of less than 0.05 was deemed significant [2]. We have found that if the primary cell was an osteoblast, then the three different experiments demonstrated similarity in the apparent diffusion coefficient (R^2/t; ANCOVA, $F_{2,44} = 0.25$, $P = 0.78$). In contrast, the experiments in which an osteoclast was the primary cell demonstrated significant difference in R^2/t between different experiments ($F_{4,22} = 4.25$, $P = 0.011$), while R^2/t remains consistent within experiments (Figure 1A; ANCOVA Interaction term, $F_{4,22} = 1.22$, $P = 0.33$).

We further investigated the dependence of R^2/t on distance from a primary cell, and found that in osteoblast experiments, it positively correlated with the distance (Figure 1B; $F_{1,44} = 8.68$, $P = 0.005$). This dependence was weaker or non-existent in different experiments in which the primary cell was an osteoclast (ANCOVA Distance factor, $F_{1,22} = 0.024$,

$P = 0.88$). We also investigated multiple peaks in $[Ca^{2+}]_i$ present in a high number of secondary responders. These peaks may result either from internally-driven oscillations or from a superposition of signals from different sources (suggesting that some of the secondary responders may in turn release the mediator). Fourier analysis demonstrated that the period

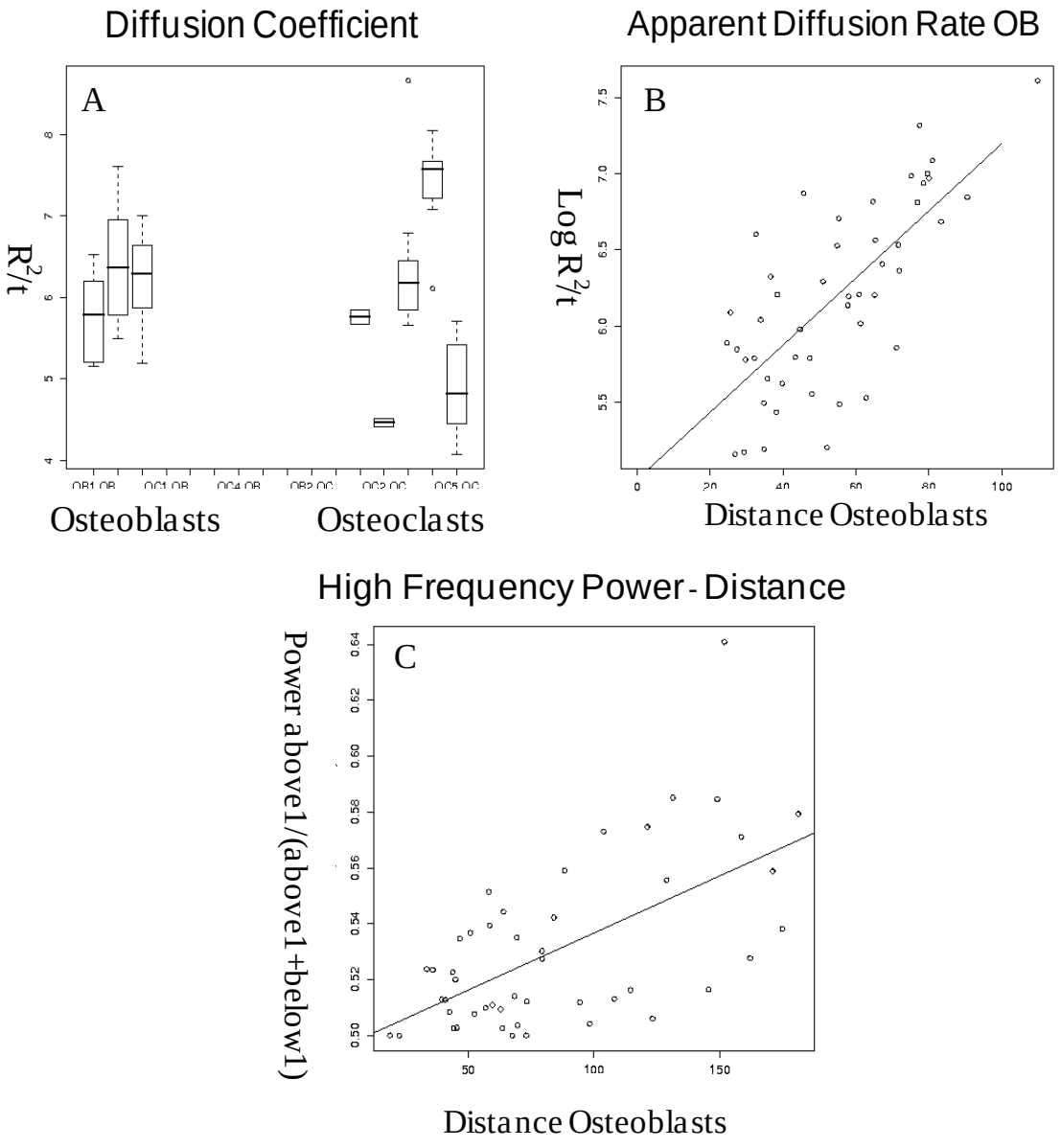

Figure 1 Data analysis of signal propagation initiated by mechanical stimulation. A) An estimate of the diffusion coefficient for 3 experiments in osteoblasts (left) and 5 experiments in osteoclasts (right). B) The relationship between the estimated diffusion coefficient and distance from the primary cell in the 3 osteoblasts experiments. C) The normalized power of the Fourier transform of the oscillatory secondary responses for frequencies above 1Hz.

between the peaks was similar in all of the experimental recordings, strongly supporting the presence of self-sustained oscillations in the secondary responders. In addition, we have found that the probability of observing an oscillatory component increases with the distance from the primary cell (Figure 1C).

Together with the increase in apparent diffusion rate, this allowed us to formulate a hypothesis that a single mediator is released from a primary cell, and subsequently starts to degrade and thus move faster as it travels further away from the source, resulting in a change in the apparent diffusion coefficient as well as the pattern of induced responses. Since a different set of data indicated that ATP is one of the potential mediators of these responses, we conjectured that ATP is released from a source cell and is degraded to ADP by extracellular nucleotidases. Whereas ATP mainly acts through P2X ligand gated ion channels, ADP only acts on P2Y G-protein coupled receptors, which accounts for the appearance of oscillations in secondary cells.

3.2 Model for combining ATP degradation and diffusion dynamics. Model assumptions are that:

1. ATP is released by a primary cell and can be degraded to ADP, which in turn degrades to AMP by extracellular nucleotidases.
2. ATP, ADP, and AMP diffuse by radial 2-dimensional diffusion with the diffusion coefficients inversely proportional to the square roots of their molecular weights, respectively.
3. ATP is released in a continuous manner over the duration of an experiment.

Then the chemical reactions are modeled by

$$\frac{\partial a_1}{\partial t} = D_1 \Delta a_1 - k_1 a_1, \tag{3.1}$$

$$\frac{\partial a_2}{\partial t} = D_2 \Delta a_2 + k_1 a_1 - k_2 a_2, \tag{3.2}$$

$$\frac{\partial a_3}{\partial t} = D_3 \Delta a_3 + k_2 a_2 - k_3 a_3, \tag{3.3}$$

where a_1, a_2, a_3 are concentrations of ATP, ADP, and AMP, respectively; D_1, D_2, D_3 are diffusion constants for ATP, ADP, and AMP, respectively [3], k_1 is a rate constant for the ATP to ADP degradation reaction, k_2 is a rate constant for the ADP to AMP degradation reaction, k_3 is a rate constant for the AMP to adenosine degradation reaction, and $\Delta = \partial^2/\partial r^2$. The parameters values were chosen based on the following experimental data: measured ATP diffusion coefficient, $D_1 = 180\ \mu\text{m}^2/\text{s}$, and estimated rate constants for the ATP to ADP and ADP to AMP reactions given by $k_1 = 0.5$ and $k_2 = 0.4$, respectively [5]. D_2 and D_3 were estimated based on the molecular weights of ATP, ADP, and AMP. We assumed that initially nucleotides are released in proportion to their concentrations in the cell, 100:10:1 for ATP:ADP:AMP [1].

When the simulations were performed for the model describing diffusion of nucleotides only ($k_1 = k_2 = k_3 = 0$), we observed that the main propagating species is ATP (Figure 2A). When we introduced the degradation of ATP to ADP ($k_1 = 0.5$, $k_2 = k_3 = 0$), the balance between the nucleotides changed as they travelled from the source, resulting in ADP becoming the main propagating species at longer distances (Figure 2B). Finally, when we added the degradation of ADP to AMP ($k_1 = 0.5$, $k_2 = 0.4$, $k_3 = 0$), then AMP became the

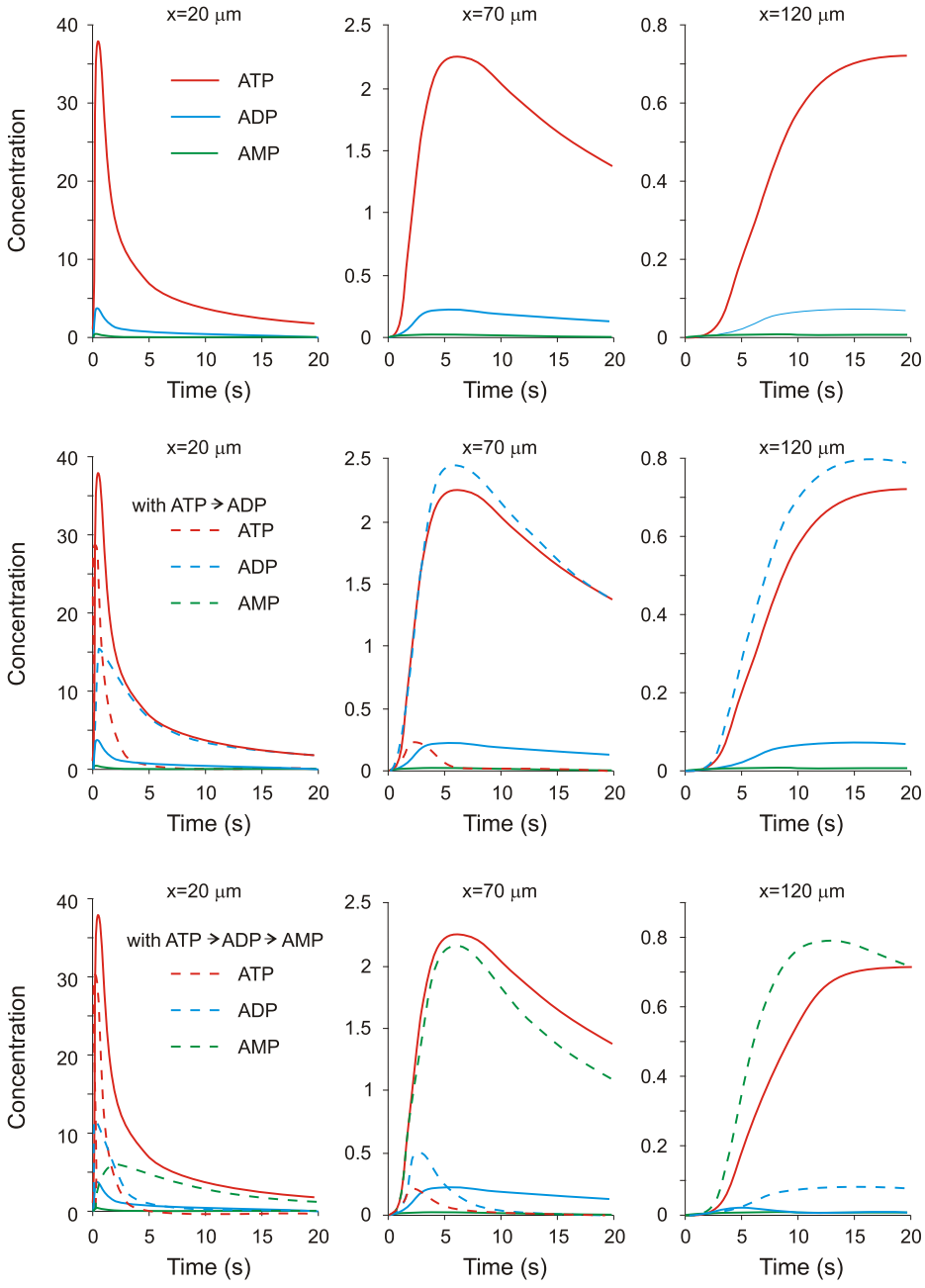

Figure 2 Changes in concentrations of ATP (red), ADP (blue), and AMP (green) at distances of 20 μm (left column), 70 μm (middle column), and 120 μm (right column) from the source, obtained from the model (3.1)-(3.3) describing: A) diffusion only (dashed lines in all figures); B) diffusion of ions and degradation of ATP to ADP; and C) diffusion of ions and degradation of ATP to ADP and ADP to AMP.

main propagating species at longer distances (Figure 2C). Thus, the model predicts that introduction of degradation of ATP to ADP is a plausible explanation for the experimentally observed increase in the value of the apparent diffusion coefficient (Figure 1B).

3.3 Model for osteoclast mediator propagation. To account for the differences observed in different experiments in which an osteoclast was stimulated, we hypothesized that since osteoclasts are vastly different in size, it is possible that the amounts of mediators released in the different experiments are quite different. This would result in significantly different contributions to the reaction time, i.e., the time needed to accumulate the required amount of a signalling molecule on the cell membrane, and to the propagation time in some of the experiments. To assess how large differences in the amount of released mediator may influence the results, the following model was built. The model assumptions are:

1. Only one mediator (with concentration $C = C(r,t)$) is released by a primary cell.
2. The mediator diffuses by 2-dimensional radial diffusion.
3. There is a threshold concentration of a mediator needed to induce a response in a secondary cell. This threshold is the same for all secondary cells.
4. The mechanical stimulation of different cells results in significantly different amounts of the mediator being released.
5. The mediator is released in a continuous manner over the duration of an experiment.

The model is simply the diffusion equation in polar coordinates with no angular dependence given by

$$D\left(\frac{\partial^2 C}{\partial r^2}+\frac{1}{r}\frac{\partial C}{\partial r}\right)-\frac{\partial C}{\partial t}=\frac{C_0}{D}\frac{\delta(r)}{r}H(t) \tag{3.4}$$

where D is the diffusion coefficient, $\delta(r)/r$ is the two-dimensional delta distribution, and $H(t)$ is the Heaviside function. This has the solution

$$C(r,t)=\frac{C_0}{4\pi D}\mathrm{Ei}\left(\frac{-r^2}{4tD}\right) \tag{3.5}$$

where Ei is the exponential integral

$$\mathrm{Ei}(-x)=-\int_x^\infty \frac{e^{-t}}{t}\,dt, \quad x>0. \tag{3.6}$$

With the substitutions $x = 1/4\pi D$ and $\alpha = r^2/t$, this can be rewritten as:

$$\frac{C}{C_0}=x\mathrm{Ei}(\alpha_{1,2}\pi x) \tag{3.7}$$

where α_1 and α_2 correspond to two values of α in each experiment. From each of two experiments, we then can compute

$$\beta(x)=\frac{C^1}{C^2}=\frac{\mathrm{Ei}(\alpha_1\pi x)}{\mathrm{Ei}(\alpha_2\pi x)} \tag{3.8}$$

where C^1 and C^2 correspond to the values of C for α_1 and α_2, respectively. The function $\beta(x)$ is plotted in Figure 3 for different values of D (180 $\mu m^2/s$ for ATP, 210 $\mu m^2/s$ for ADP). The model predicts that if the propagating species is ATP, with diffusion coefficient of 180 $\mu m^2/s$, then two specific ratios of C^1/C^2 will be predicted and observed at the same value of D in the experiments. Since ATP can be experimentally measured [6], the hypothesis can be tested in the future.

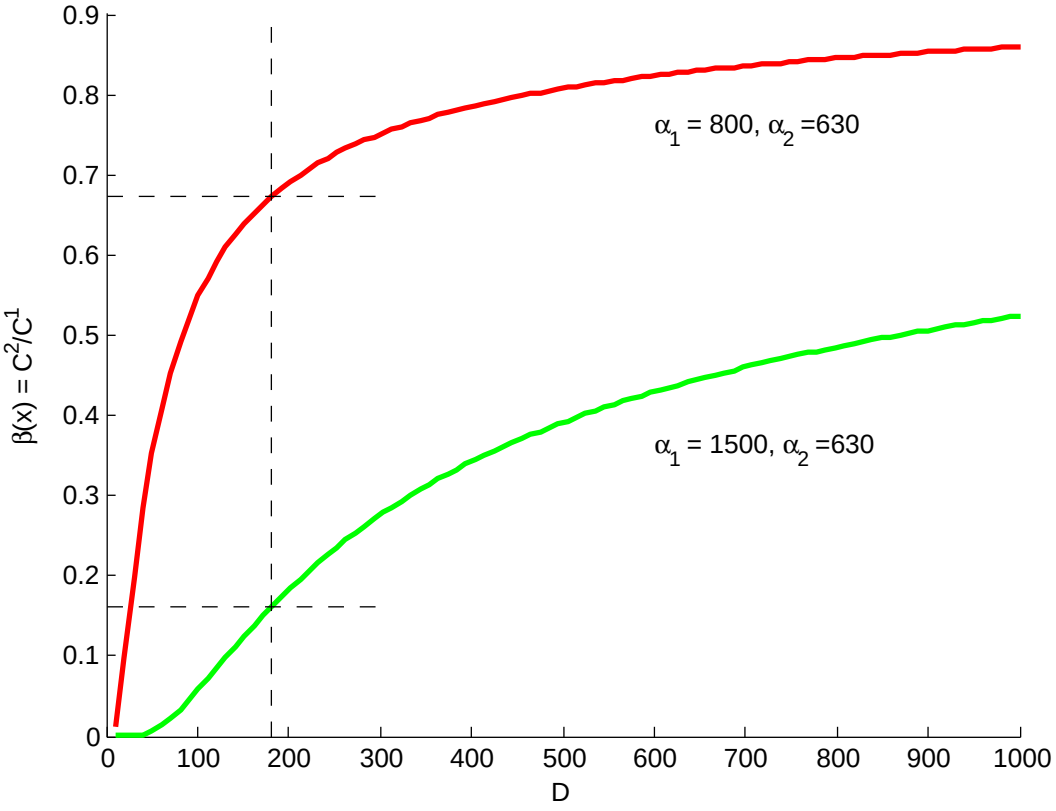

Figure 3 The function $\beta(x)$ is plotted for 2 sets of experiments in each of which α_1 and α_2 were measured. If ATP is the main mediator of the response, then the C^2/C^1 ratio also can be estimated for each experiment and they should intersect the $\beta(x)$ axis at the locations corresponding to the known value for the diffusion coefficient of ATP.

4 Conclusions

This study has allowed us to conclude the following:

1. A mediator is released from a single source cell.
2. The response to the mediator changes with distance.
3. The value of the apparent diffusion coefficient increases with distance.
4. A plausible proposed mechanism is that ATP is released and degrades to ADP.
5. Future experiments are required to confirm that ATP is the mediator as suggested.

References

[1] F.I. Ataullakhanov and V.M. Vitvitsky, *What determines the intracellular ATP concentration*, Biosci. Rep. **22** (2002), no. 5-6, 501–511.

[2] M. Evans, N. Hastings, and B. Peacock, *Statistical Distributions, 3rd Edition*, John Wiley and Sons, 2000.

[3] S.T. Kinsey and T.S. Moerland, *Metabolite diffusion in giant muscle fibers of the spiny lobster Panulirus argus*, J. Exp. Biol. **205** (2002), 3377–3386.

[4] A. Liedert, D. Kaspar, R. Blakytny, L. Claes, and A. Ignatius, *Signal transduction pathways involved in mechanotransduction in bone cells*, BBRC **349** (2006), no. 1, 1–5.

[5] P. Meghji, J.D. Pearson, and L.L. Slakey, *Kinetics of extracellular ATP hydrolysis by microvascular endothelial cells from rat heart*, Biochem J. **308** (1995), 725–731.
[6] I.R. Orriss, G.E. Knight, J.C. Utting, S.E. Taylor, G. Burnstock, and T.R. Arnett, *Hypoxia stimulates vesicular ATP release from rat osteoblasts*, J. Cell Physiol. **220** (2009), no. 1, 155–162.
[7] D. Taylor, J.G. Hazenberg, and T.C. Lee, *Living with cracks: damage and repair in human bone*, Nature Materials **6** (2007), no. 4, 263–268.
[8] C.H. Turner, *Bone strength: current concepts*, Ann. N.Y. Acad. Sci. **1068** (2006), 429–446.